Supplementary Material

Supplementary A: AAR deployment sites, detection ranges and the Bengulea environment

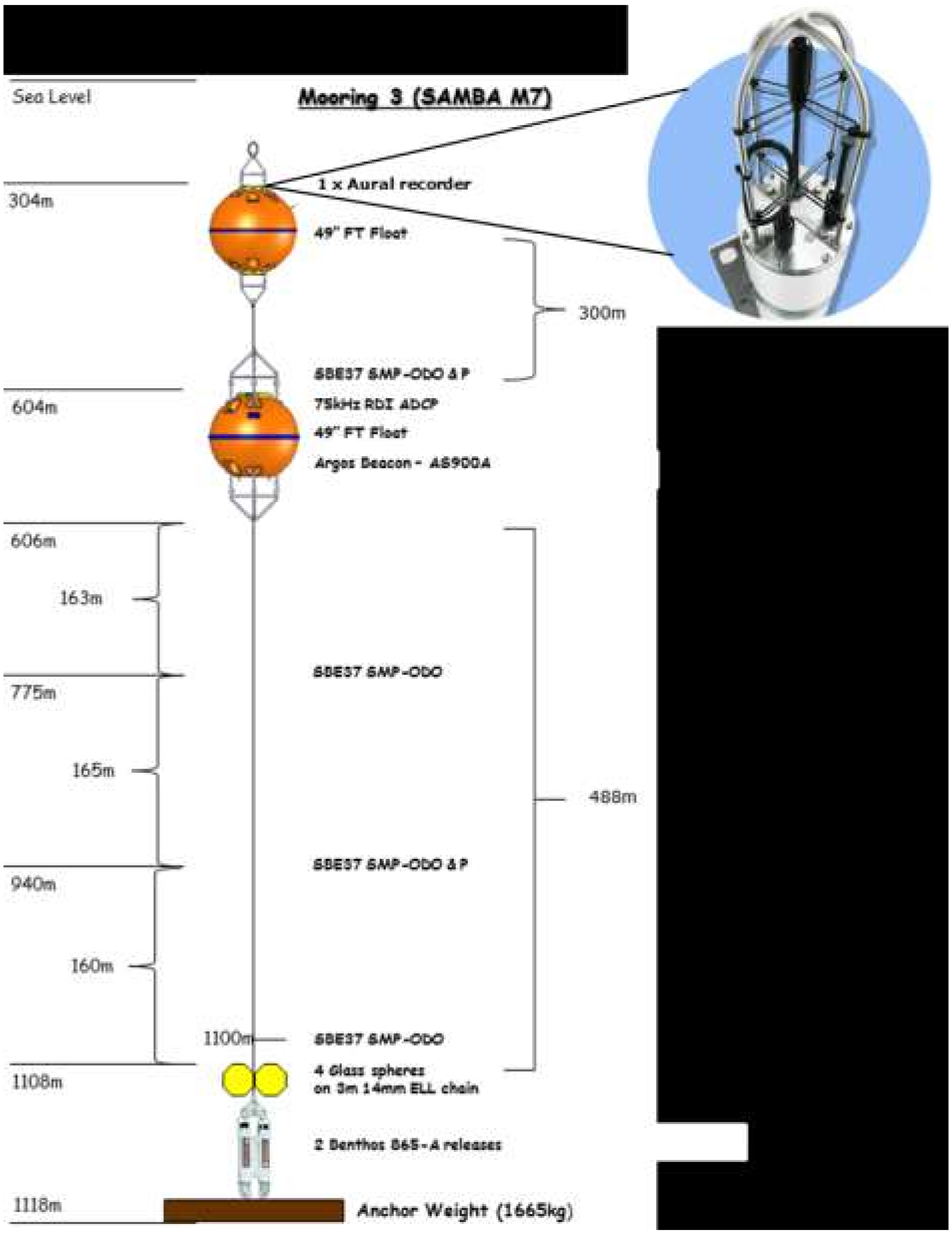

Supplementary Figure S1. Schematic representation of one of the SAMBA oceanographic moorings showing the position of AAR2 on the top buoy/float. The inset provides a magnified view of the hydrophone and protective bars on the AAR's head. Different oceanographic instruments are also seen attached at different depths of the mooring below the top buoy.

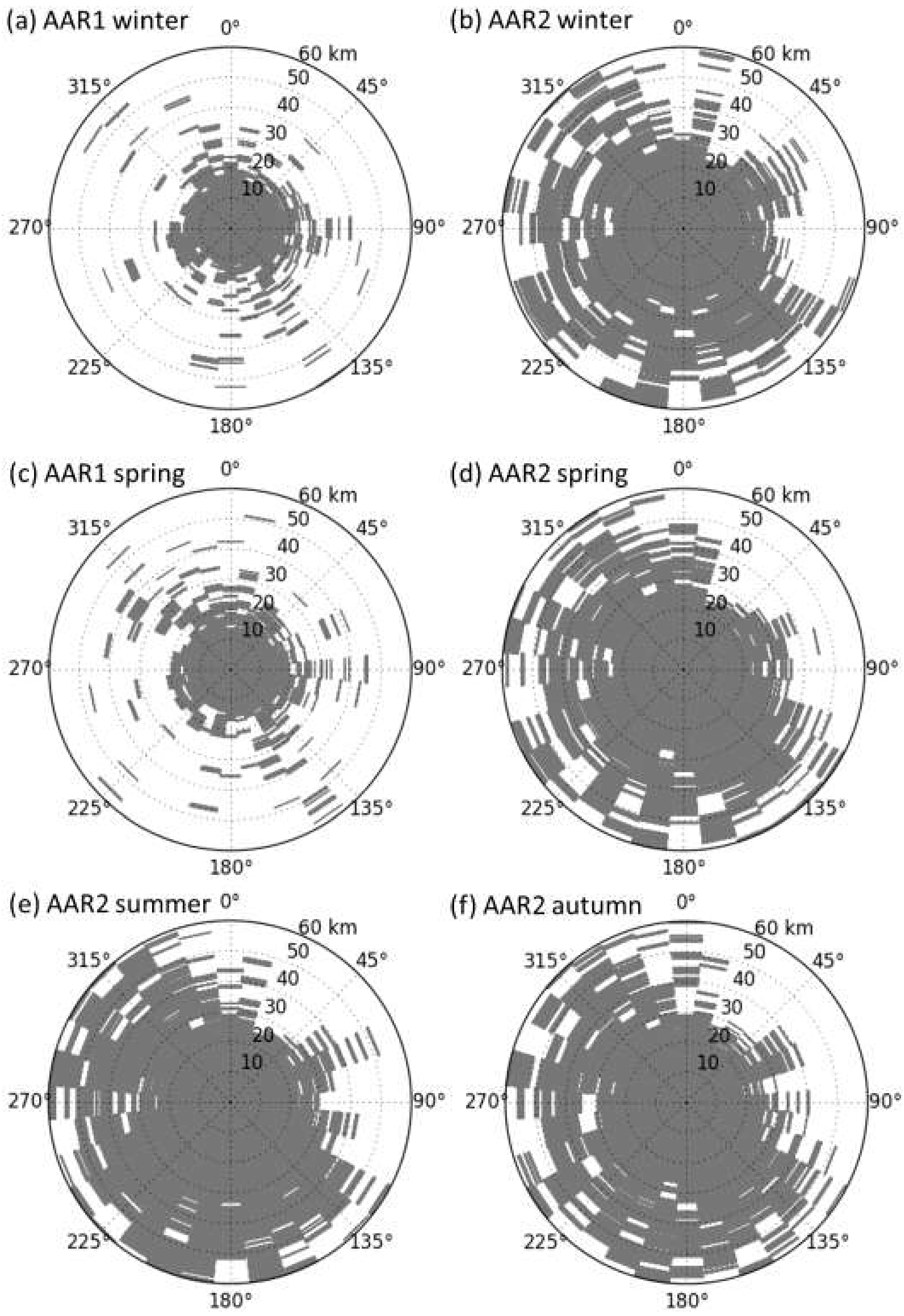

Supplementary Figure S2. Polar plots showing seasonal detection ranges for Antarctic blue and fin whale calls between AAR1 (a and c) and AAR2 (b, d, e and f) at different bearings. No acoustic data were collected during summer and autumn for AAR1. Grey patches denote regions from which a call would be detectable at the hydrophone location (centre of plot).

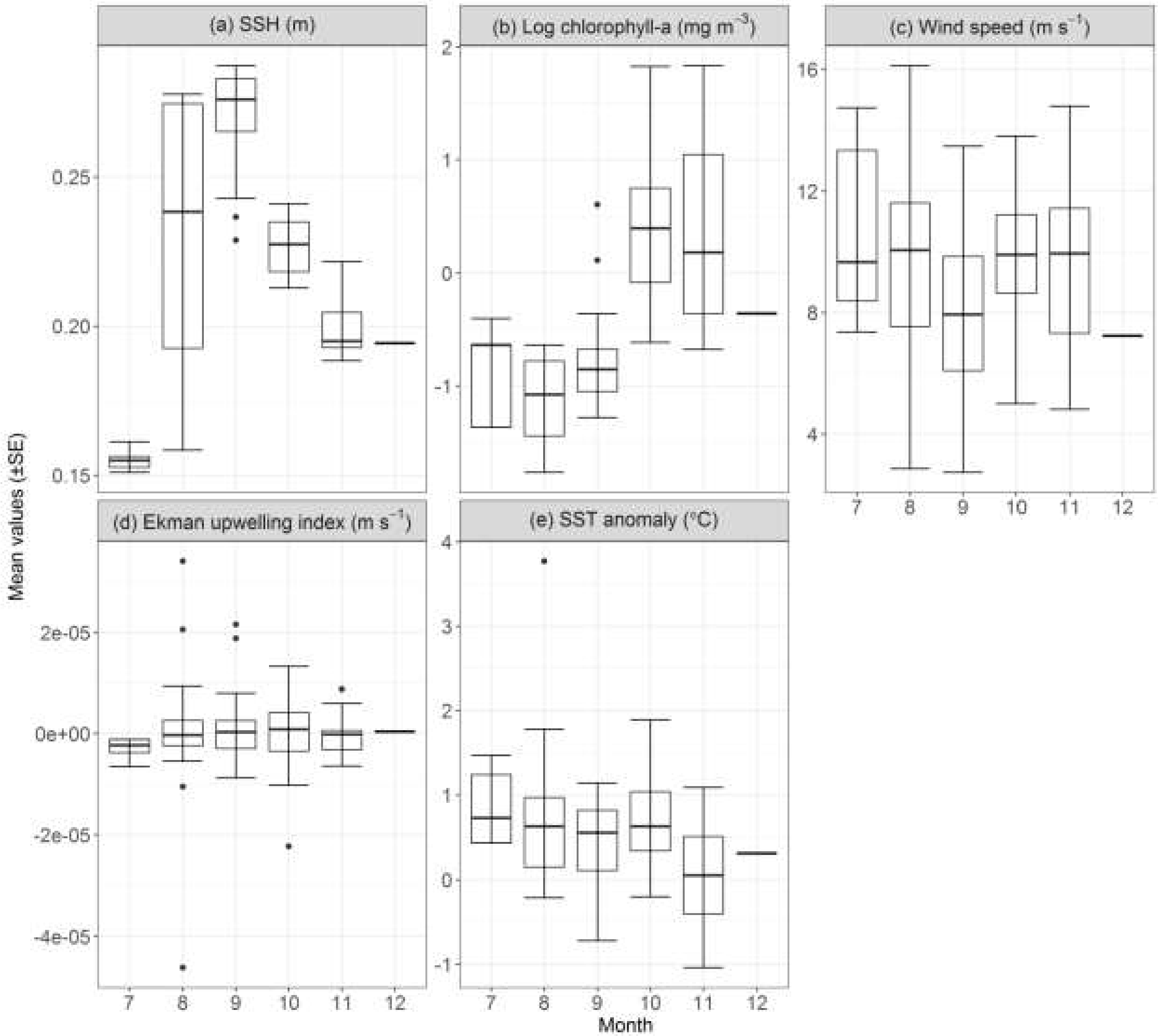

Supplementary Figure S3. Box and whisker plots showing trends of the five different environmental variables around AAR1 location. The box represent the first quartile to the third quartile (the interquartile range), and the segment inside the box is the median. The whisker delineates 1.5 times the interquartile width, and the closed circles are observations that are outside the range covered by the whisker.

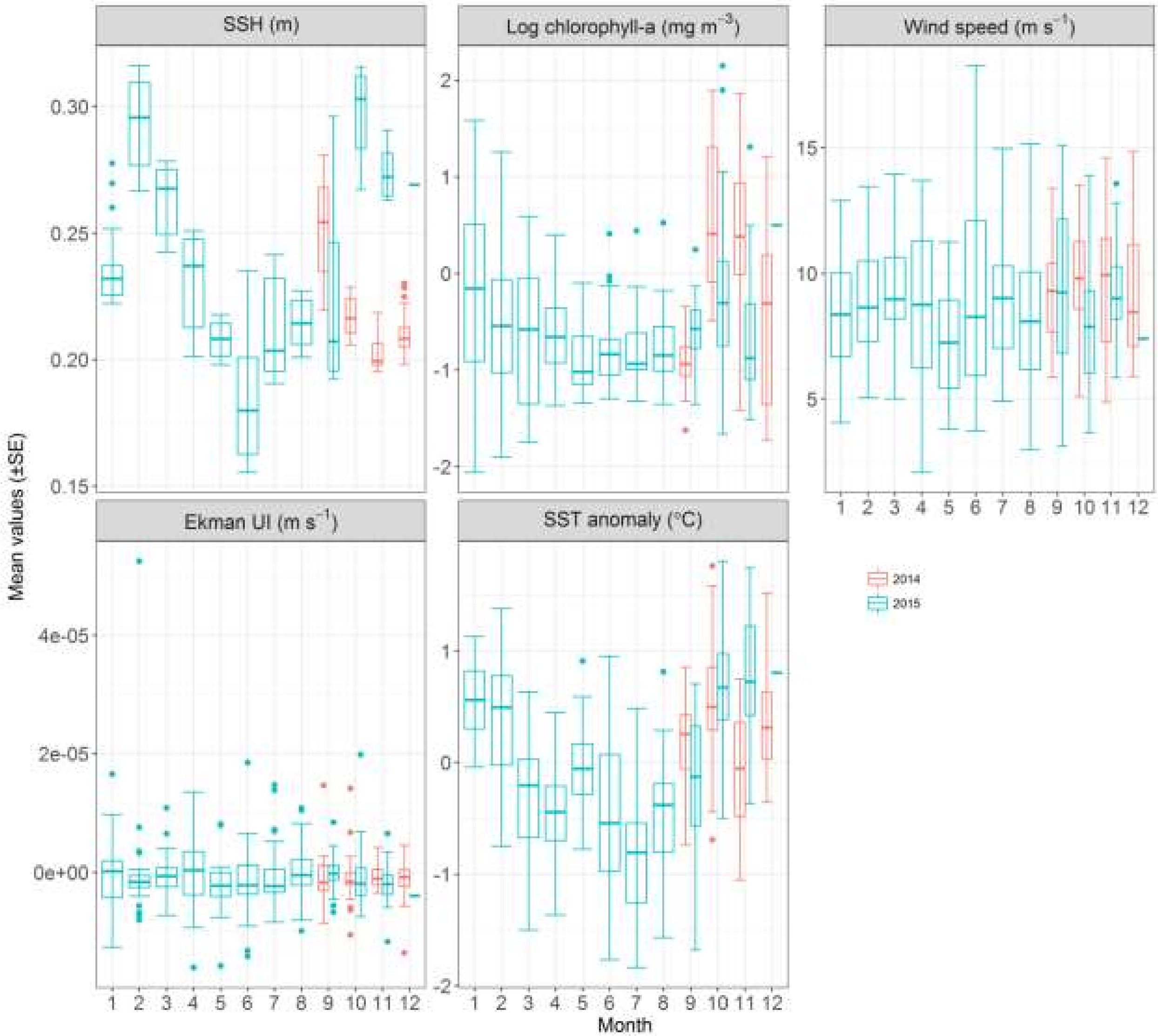

Supplementary Figure S4. Box and whisker plots showing trends of the five different environmental variables around AAR2 location. The box represent the first quartile to the third quartile (the interquartile range), and the segment inside the box is the median. The whisker delineates 1.5 times the interquartile width, and the closed circles are observations that are outside the range covered by the whisker.

Supplementary B: Method on diel call rates and smoothing

Different light regimes for plots were classified over different seasons in accordance with the altitude of the sun (dawn (nautical twilight), daytime, dusk (nautical twilight) and nighttime) by averaging hourly sun altitudes over austral seasons. We used hourly sun altitudes for each day of the year from 34° 22"S, 17° 37"E for both AAR locations since there should be no difference in the light conditions between the two closely spaced locations. Sun altitudes were obtained from the United States Naval Observatory Astronomical Applications Department (http://aa.usno.navy.mil). We defined the nautical dawn hours as periods when the centre of the sun was geometrically 12° below the horizon before sunrise. Daytime hours were between sunrise and sunset, and the nautical dusk hours were between sunset and the evening. Nighttime hours were instants when the geometric centre of the sun was 12° below the horizon in the evening, which is between dusk and dawn.

AAR1 smoothed means of diel call rate patterns per season for plots were calculated by fitting GAM using a smooth term that specified penalized cyclic cubic regression splines as a circular averaging. Smoothed means of the diel call rate patterns per season for plots from AAR2 were calculated through penalized cyclic cubic regression splines in GAM.

Supplementary C: Comparing RF model with GAM and GBM

Two different ways of assessing model performance were used for count (presence and absence) and continuous (call rates) data. The area under the receiver operating characteristic curve (AUC) was used to measure the predictive accuracy of our RF classification model compared to GAM and GBM, i.e. how well the model correctly classified the classes included in the model (here the presence and absence of whale calls). AUC normally takes values between 0.5 and 1, where values closer to 1 indicate better classification ability (DeLong et al., 1988). The number of replicates was set to 200 for the model performance assessment. Using 80% of the data for training and the remaining for validation, the performances of GAM, GBM and RF models for Antarctic blue and fin whale call rates modelling were assessed. Root mean square prediction error (RMSPE) was used to measure the difference between values predicted by the model and observed values (e.g. Chai and Draxler, 2014). In addition, Spearman's rank correlation coefficient (rho) was applied as a qualitative measure of the performance of models. A low RMSPE value indicates a better model and the opposite is true for rho.

Only the RF model was better at detecting statistical signals and had higher prediction accuracy than GBM and GAM as it had higher AUC values (Supplementary Table S1) for both AARs. The correlations between the predicted and observed values of all three call rates were also highest for RF model (Supplementary Table S2) in both systems. RF model optimal parameter configurations are provided in Supplementary Table S3.

Supplementary Table S1. Model performance outcomes between GAM, GBM and RF for acoustic seasonal occurrences of Antarctic blue and fin whales according to AUC from AARs 1 and 2. SD is the standard deviation. Boldface indicates values of a model with better performance.

		GAM		GBM		**RF**	
AAR	Species type	Mean	SD	Mean	SD	Mean	SD
AAR1	Blue whale	0.843	0.011	0.766	0.043	**0.872**	**0.034**
	Fin whale	0.839	0.101	0.839	0.033	**0.881**	**0.087**
AAR2	Blue whale	0.946	0.021	0.870	0.033	**0.958**	**0.012**
	Fin whale	0.848	0.006	0.848	0.006	**0.967**	**0.009**

Supplementary Table S2. Model performance outcomes between GAM, GBM and RF for Antarctic blue and fin whale call rates from AARs 1 and 2 based on root mean square prediction error (RMSPE) and Spearman's rank correlation coefficient (rho). Boldface indicates values of a model with better performance.

		rho		RMSPE	
AAR	Call-model types	Mean	SD	Mean	SD
AAR1	F-GAM	0.114	0.023	0.434	0.034
	F-GBM	0.136	0.035	0.439	0.039
	F-RF	**0.137**	**0.017**	**0.362**	**0.043**
	Z-GAM	0.269	0.016	0.681	0.021
	Z-GBM	0.221	0.024	0.712	0.026
	Z-RF	**0.323**	**0.015**	**0.613**	**0.026**
AAR2	D-GAM	0.024	0.016	0.100	0.019
	D-GBM	0.034	0.030	0.104	0.019
	D-RF	**0.041**	**0.009**	**0.099**	**0.016**
	F-GAM	0.349	0.007	1.021	0.013
	F-GBM	0.404	0.011	1.241	0.021
	F-RF	**0.488**	**0.028**	**0.753**	**0.017**
	Z-GAM	0.309	0.008	0.637	0.009
	Z-GBM	0.341	0.013	0.725	0.015
	Z-RF	**0.385**	**0.018**	**0.508**	**0.013**

Supplementary Table S3. Optimal parameter configuration values used in the RF model to investigate seasonal call occurrences and call rates from AARs 1 and 2. Mtry is the number of variables randomly selected at each tree node; ntrees is the number of growing trees, nodesize is the splitting minimum size of terminal nodes of trees, Z is Z-call rates, D is D-call rates, F is fin whale call rates, BP is Antarctic blue whale presence, and FP is fin whale presence.

AAR	Mtry	Ntrees	Nodesize	Group
AAR1	4	1500	1	Z
	3	1000	1	F
	1	1500	1	BP
	1	500	1	FP
AAR2	1	500	1	Z
	1	500	5	D
	2	500	1	F
	1	3000	1	BP
	1	2500	1	FP

Supplementary D: Results of diel call occurrences and call rates

Both blue and fin whale call occurrence was greatest in winter for both AARs (Supplementary Figure S5). For AAR1, the proportion of call occurrence for Antarctic blue whales peaked during daytime in winter and spring (Supplementary Figure S5); there were also some peaks of blue whale call occurrence at night in winter and spring. For AAR2, the proportion of call occurrence for Antarctic blue whales peaked during daytime in autumn and winter (Supplementary Figure S5); blue whale call occurrence only peaked at night in spring. High Z-call rates of Antarctic blue whales from AAR1 were recorded during daytime in winter whilst more calls were recorded after mid-night in spring (Supplementary Figure S6a and b). For AAR2, autumn and winter had flat Z-call rates throughout the day and night, whereas high Z-call rates were recorded during nighttime in spring (Supplementary Figure S6c-e). D-call rates increased after midday to midnight in winter and no calls were recorded in other seasons (Supplementary Figure S6f).

The proportion of fin whale call occurrence from AAR1 peaked before dawn to midday in spring, and fin whale call occurred at night to early morning during winter (Supplementary Figure S5). In winter, the proportion of fin whale call occurrence for AAR2 peaked from midnight to dawn but decreased in the early morning; occurrence increased again from midday to dusk with a slight decrease after dusk and increased again towards mid-night (Supplementary Figure S5). In autumn and spring, fin whale calls from AAR2 occurred more during dawn and daytime (Supplementary Figure S5). Fin whale call rates from AAR1 decreased from midnight to mid-day and slightly increased after dawn in winter but peaked at dawn and dusk in spring (Supplementary Figure S6g and h). Fin whale diel call rates from AAR2 were flat during spring; call rates peaked after midnight to midday in winter but peaked from midnight to early morning in spring (Supplementary Figure S6i-k). Flat diel call rates during certain seasons of the year indicate that GAM didn't find any significant difference between different times of the day.

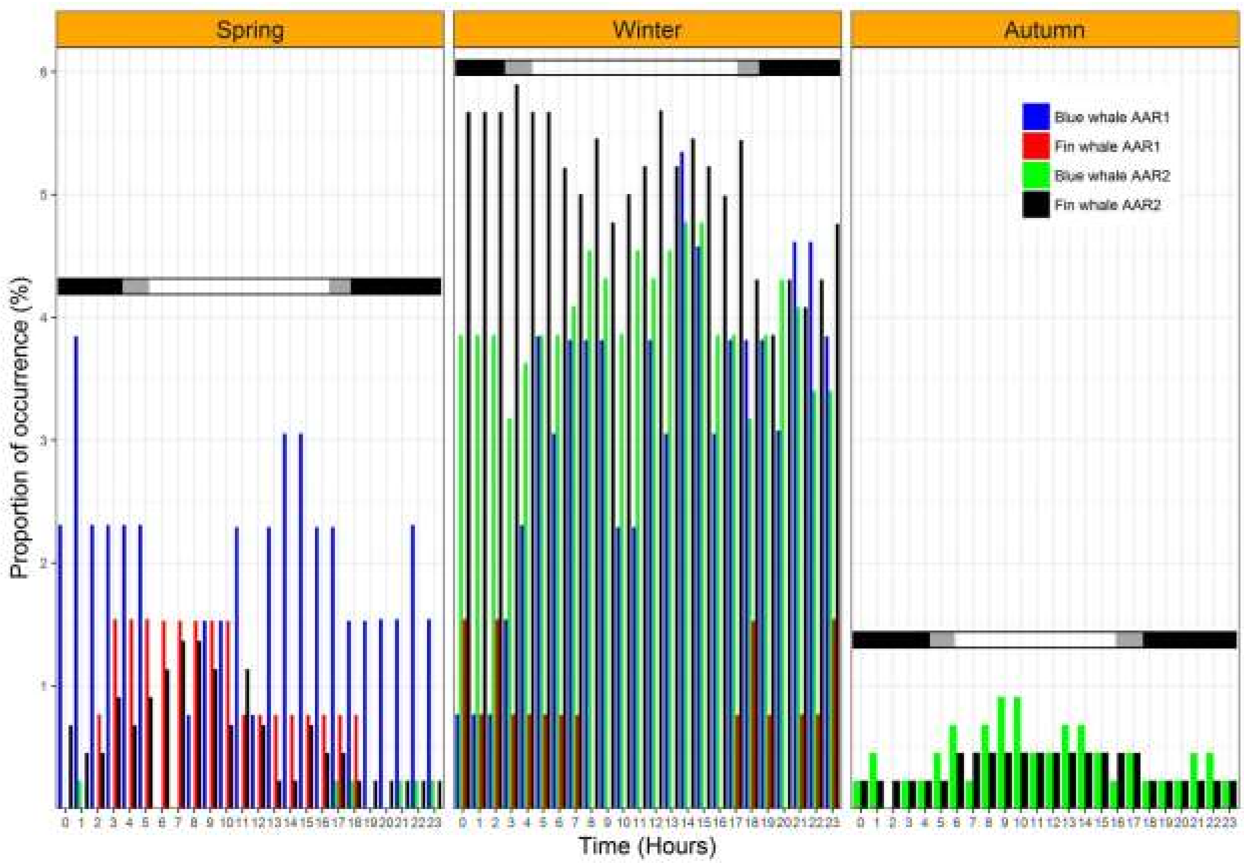

Supplementary Figure S5. Diel proportion of call occurrence per season for Antarctic blue and fin whales off the west coast of South Africa. Horizontal diel bar shading: black represents average nighttime hours, grey represents average twilight hours and white represents average daytime hours. For AAR1, no recordings were made in autumn.

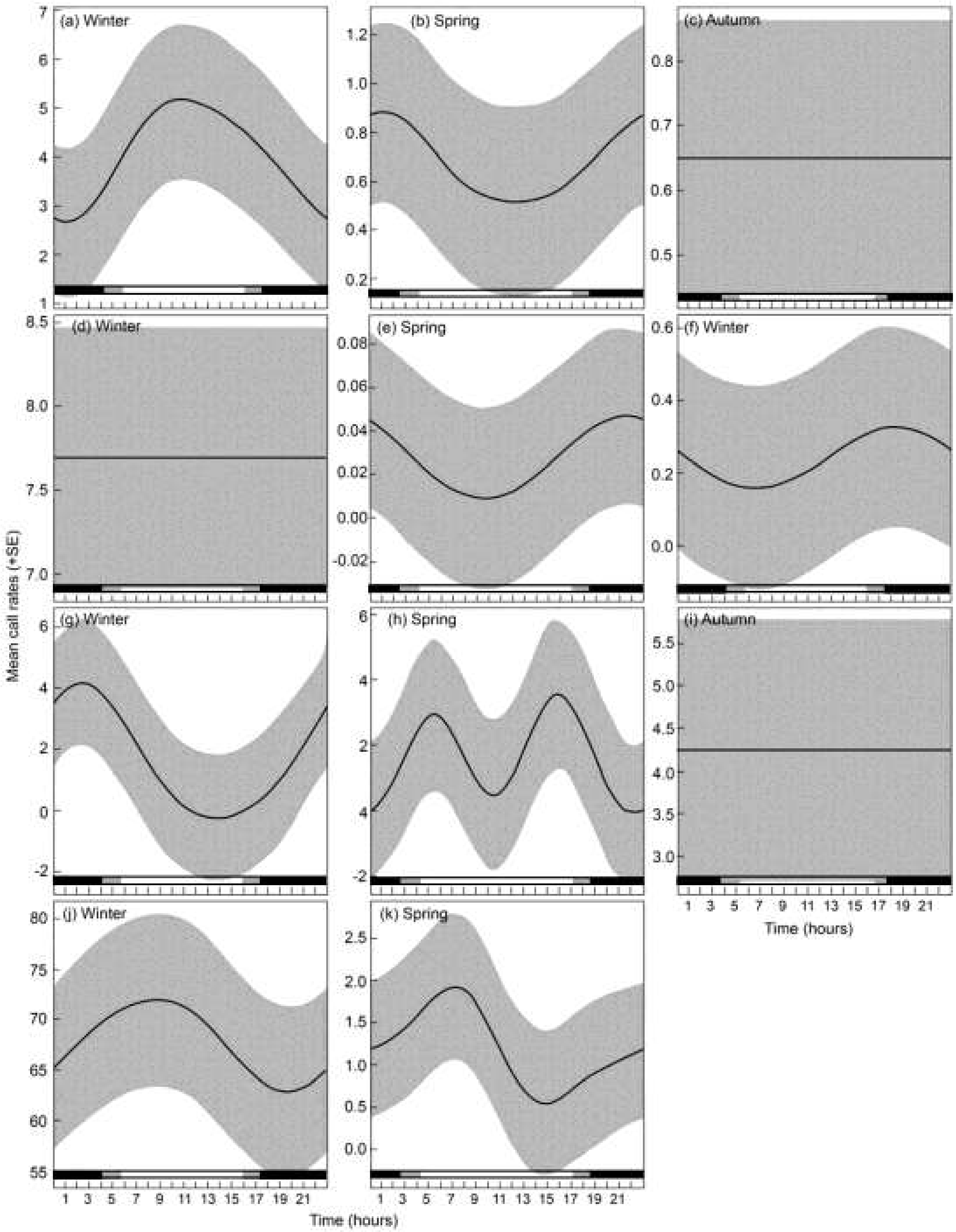

Supplementary Figure S6. Circular smoothed mean diel call rate patterns per season of Antarctic blue and fin whale off the west coast of South Africa. (a)-(b) Z-call rates in winter and spring respectively from AAR1; (c)-(e) diel Z-call rates in autumn, winter and spring respectively from AAR2; and (f) diel D-call rates in winter from AAR2. (g)-(h) Diel fin whale call rates in winter and spring respectively from AAR1; (i)-(k) diel fin whale call rates in autumn, winter and spring respectively from AAR2. The grey shaded areas of the line plot indicate the standard error (SE) of the smoothed mean (line). Horizontal diel bar shading: black represents average nighttime hours, grey represents average twilight hours and white represents average daytime hours.

Supplementary References

Chai, T., and Draxler, R.R. 2014. Root mean square error (RMSE) or mean absolute error (MAE)? – Arguments against avoiding RMSE in the literature. Geoscientific Model Development 7: 1247–1250.

DeLong, E.R., Delong, D.M., and Clarke-Pearson, D.L. 1988. Comparing areas under two or more correlated Receiver Operating Characteristic curves: a nonparametric approach. Biometrics, 44(3): 837–845.